DESIGN AND CYTOCOMPATIBILITY OF HYALURONIC ACID HYDROGELS FOR BONE REGENERATION

by

IRELAND D. JOHNSON

A THESIS

Presented to the Department of Biology
and the Robert D. Clark Honors College
in partial fulfillment of the requirements for the degree of
Bachelor of Science

March 2022

THESIS DEFENSE COMMITTEE APPROVAL

Approved: _____ Date: 03/08/2022
Dr. Marian Hettiaratchi, Primary Thesis Advisor

Approved: _____ Date: 03/08/2022
Dr. Daniel Grimes, Second Reader

Approved: _____ Date: 03/08/2022
Dr. Daphne Gallagher, Honors College Thesis Advisor

An Abstract of the Thesis of

Ireland Johnson for the degree of Bachelor of Science
in the Department of Biology to be taken March 2022

Title: DESIGN AND CYTOCOMPATIBILITY OF HYALURONIC ACID BASED HYDROGELS FOR BONE REGENERATION

Large bone defects and fractures caused by trauma or disease remain a serious challenge for orthopedic surgeons and there is a need for more effective treatment strategies to repair injured bone. Bone autografts, a tissue graft from the same patient, are the ideal treatment strategy because there is a low chance of host rejection, and the graft is not weakened from sterilization. However, bone autografts are not widely available, and their harvest can cause donor site morbidity. As an alternative strategy, biomaterials composed of the natural polymer hyaluronic acid (HA) can be used to deliver osteogenic (bone-forming) proteins that repair injured bone. The objective of this study was to develop and test the cytocompatibility of HA-based hydrogels for protein delivery for bone regeneration applications. HA hydrogels were formed by dynamic, covalent bonds between aldehyde functional groups on oxidized HA and HA functionalized with adipic acid hydrazide or carbohydrazide groups. Hydrogels were seeded with 3T3 fibroblast cells to evaluate cell compatibility. Live and dead cells were evaluated using green fluorescence from GFP and red fluorescence from ethidium homodimer, respectively. A combination of HA separately modified with oxidized and carbohydrazide HA, each at 2.5% (w/v), maintained high cell viability (>82.3% for all time points) and encouraged a rate of cell growth that surpassed all other conditions. This project also investigates the cytocompatibility of the HA hydrogels with skeletal

myoblasts. Future work will aim to further functionalize and optimize the HA hydrogels themselves as a protein delivery vehicle for osteogenic proteins like bone morphogenetic protein 2. The impact of this project will facilitate the future use of HA hydrogels as a biomaterial that rivals the healing response of bone autografts.

Acknowledgements

First and foremost, I would like to express my deep and sincere gratitude to Dr. Hettiaratchi for helping me dive into the field of bioengineering. She motivated me to dream bigger and reach for goals I didn't think I was capable of. I will always be incredibly grateful for her support and guidance.

I would also like to thank Veronica Spaulding for her patience and always answering every one of my questions, Annie Gilbert for introducing me to the world of MSCs and Dr. Kaitlin Fogg for guiding me through cellular image analysis. I would like to acknowledge members of the Hettiaratchi Lab and others for their support and guidance over the past two years, including Jonathan Dorogin, John O'Hara-Smith, Hossein Rajabzadeh, Henry Hochstatter, Yan Carlos Pacheco, Chandler Asnes, Lily Mozipo, Simon Oh, Angela Lin and Kelly Leguineche. I am extremely grateful to Dr. Marian Hettiaratchi, Dr. Daniel Grimes and Dr. Daphne Gallagher for their time and serving on my thesis committee. Thank you to the Knight Campus Undergraduate Scholars Program and the Peter O'Day Fellowship Program for providing funding to my undergraduate research career.

In addition, I would like to thank Haley Landis, who provided happy distractions, shared her excellent music taste, and participated in late night dance sessions with me over the past two years. Lastly, I want to extend my appreciation and thanks to Alexander Binder, without whose never-failing support, I wouldn't have been able to laugh while climbing mountains and write this thesis at the same time.

Table of Contents

Introduction

Large bone defects and fractures caused by trauma or disease remain a serious challenge for orthopedic surgeons. Six million bones are fractured annually in the United States and in cases of trauma-based fractures, 82% require surgery (Somersalo et al., 2014). Many tissue injuries, like critically sized bone defects, do not readily heal without medical intervention. There is a need for more effective treatment strategies to repair injured bone. Clinically, one of the most frequently used strategies is bone allografts, a tissue graft from a donor individual, which can trigger tissue rejection, especially in younger patients (Barrett et al., 2011). The sterilization process, which includes high-dose radiation, can also damage the integrity of the donor tissue (Awad et al., 2007). However, allografts are widely available and significantly more affordable. Bone autografts, a tissue graft from the same patient, are an ideal treatment strategy, and are often referred to as the "gold standard," because there is a low chance of host rejection, and the graft is not weakened from sterilization (Awad et al., 2007). However, bone autografts are difficult to obtain, their harvest can cause donor site morbidity and they can pose great financial strain on the patient (Kassir & Chakar, 2018). Many researchers are looking for alternate strategies and methods to develop a new treatment that rivals the healing response of a bone autograft.

Biomaterials

Biomaterials, composed of a variety of compounds or polymers and intended for implantation in tissue, are used medically in everything ranging from pacemakers to contact lenses to orthopedic devices. We are interested in developing hydrogels, a subgroup of biomaterials, for bone regeneration applications. With proper development

and modification, hydrogels can be used to deliver osteogenic proteins that stimulate a healing response (Hettiaratchi et al., 2020). Previous research has indicated that fibrin hydrogels paired with growth factor delivery systems promoted the regeneration of bone tissue (Schmoekel et al., 2005). Growth factor functionalized hydrogels have shown significant cytocompatibility in vivo and improved localized bone regeneration (Lienemann et al., 2012). Additionally, research with hyaluronic acid hydrogels has indicated that they are hydrolytically stable and are capable of tissue adhesive properties (Bermejo-Velasco et al., 2019).

Hydrogels are composed of polymers that form network structures when crosslinked (Figure 1) via covalent or noncovalent interactions (Dorogin et al., 2021). Natural polymers are typically cytocompatible, as the polymers resemble native extra cellular matrices found in biological systems and, in some instances, have the potential to exhibit osteoinductive properties (Haugen et al., 2019). Some hydrogels, once crosslinked, do not dissolve when exposed to natural tissue, proteins, or cells, while others degrade over time. Ideally, hydrogels dissolve as they are replaced by regenerated tissue (Hozumi et al., 2018). They are also modifiable, and thus

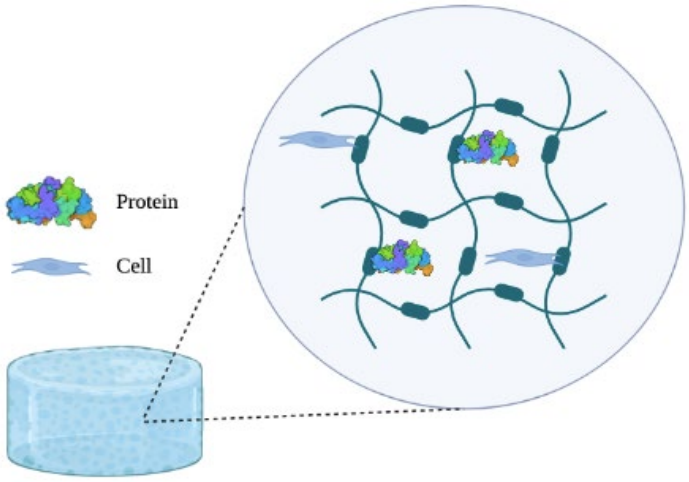

Figure 1. Schematic of hydrogel depicting proteins and cells encapsulated within the crosslinked network. Figure adapted from Veronica Spaulding and created with BioRender.com.

tunable, making them versatile for many different types of applications (Muir & Burdick, 2021). Different types of cells, drugs and proteins can be encapsulated into the hydrogels due to their high water content (Yu & Ding, 2008). Like many applications of hydrogels, bone regeneration applications use hydrogels as a tunable scaffold that can facilitate and promote the growth and development of new bone.

Polymer Types

The use of different polymers allows for different features, such as the hydrogel swelling ratio, degradation rate, gelation time, Young's modulus, and cytotoxicity. The swelling ratio is the normalized increase in the mass of the hydrogel after it absorbs water. This ratio can affect the transport and delivery of proteins and drugs and influence the proliferation and differentiation of cells (Park et al., 2009). The degradation rate is the rate at which hydrogels naturally dissolve over time, which is highly dependent on the specific polymer network and crosslinking method used. The ability to control the degradation rate of hydrogels allows researchers to specialize hydrogels to different applications, such as cartilaginous tissue formation or bone regeneration. The length of time a hydrogel should be present in a body system is different for each application (Kong et al., 2004). Gelation time is the duration it takes for polymers to crosslink and the hydrogel to solidify, which can occur over a range of seconds to hours (Patenaude et al., 2014). Young's Modulus is used to analyze the stiffness of a material with compression testing, this feature can also be modified for different applications. In some cases, it would be beneficial to match the stiffness of a hydrogel to its application site, as to better mimic the natural environment. There are limitations in the range of stiffness a hydrogel can exhibit. For example, it is very

difficult to engineer a hydrogel that can match the stiffness of bone, but far easier to create a hydrogel that can mimic the stiffness of softer tissues, like muscle fibers or blood vessels.

One polymer commonly used in hydrogels is collagen (including types I, II and III). It is found naturally in the body and comprises 90% of the proteins in connective tissues (Antoine et al., 2014). It is found in tendons, muscles, bones, organs, skin, blood vessels and other tissues. It functions to provide mechanical support and orient diverse cell types. Collagen presents low antigenicity, a low inflammatory response, adequate biodegradability, and biocompatibility (Antoine et al., 2014). Collagen hydrogels physically crosslink at 37 ºC, resulting in poor mechanical strength. Additionally, the natural degradation products of collagen are amino acids that can activate the coagulation cascade. In addition, the price of collagen does not prove to be cost effective on a large scale (Catoira et al., 2019).

Gelatin, or denatured collagen, is another natural polymer frequently used in hydrogels. It has minimal immunogenicity and is frequently used to enhance cell attachment in vascular tissue regeneration (Fu et al., 2014). Since it has stability in a wide range of pH values and at high temperatures, these features allow gelatin to be combined with other polymers for additional tunability (Catoira et al., 2019). Fibrin, a protein typically involved blood clotting, has similar properties to collagen, leading to potential regenerative applications. With its extensive fiber network, research suggests that cells grown in fibrin hydrogels produce more collagen and elastin, important components of the extracellular matrix, than cells seeded into other hydrogels (Kim et

al., 2007). Additionally, research has indicated that fibrin hydrogels could rival the response of a bone autograft (Chrobak et al., 2017).

Hyaluronic acid (HA) is a glycosaminoglycan, composed of a long, repeating chain of disaccharide units (Figure 2). With the addition of different functional groups, leading to high tunability, HA can form the extracellular matrix network. In its natural form, it is biodegradable, biocompatible, non-immunogenic and can be absorbed through multiple metabolic pathways (Muir & Burdick, 2021). HA modified with different functional groups are chemically crosslinked together forming hydrogels with different, unique properties. By varying the molecular weight and functional groups on HA, it is possible to tune the degradation time, gelation time and stiffness of HA hydrogels (Xu et al., 2020). This modification also allows for hydrogel injectability, tunability of various mechanical properties and protein binding and release (Muir & Burdick, 2021). Since HA is a chain of repeating units, each of these individual units can be modified individually thus, it is possible to have multiple osteogenic protein

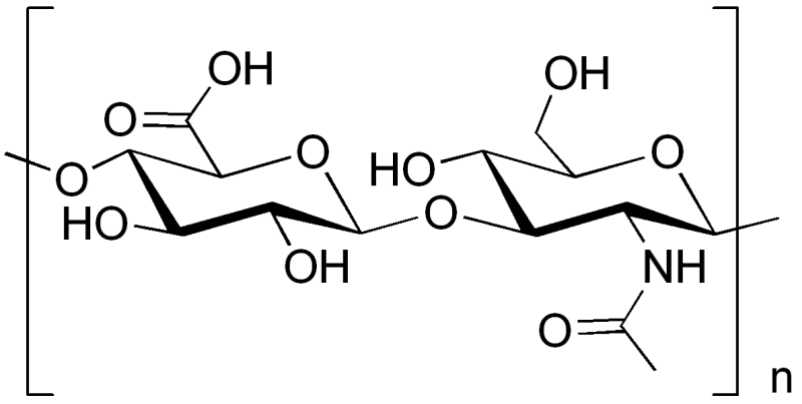

Figure 2. Molecular Structure of a Single Unit of Hyaluronic Acid. Full chain and hydrogel would consist of multiple specific repeating units.

binding sites within one hydrogel, allowing for maximum osteogenic healing response.

Due to the high tunability potential of HA, it is an ideal hydrogel for bone regeneration applications.

Crosslinking Methods of Hyaluronic Acid

Through the dynamic covalent bonds (bonds that can switch between molecules) between aldehyde and hydrazide functional groups modified onto the HA, hydrogels can be formed (Muir & Burdick, 2021) (J. Xu et al., 2019) (Wang et al., 2018). The oxidized HA (top structure of Figure 3) undergoes a ring break that allows covalent binding between the hydrazide HA (bottom structure of Figure 3). This depiction is generalized, and with different modifications on the HA, this can result in slightly different placements of crosslinking.

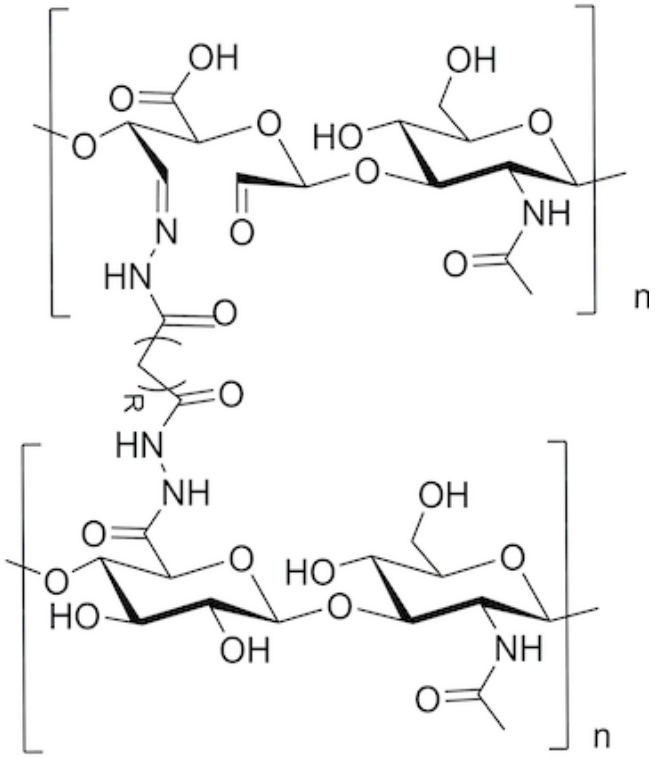

Figure 3. Depiction of crosslinking method between two functionalized hyaluronic acid polymers, oxidized and carbohydrazide, to form a hydrogel.

Relevant Cells

Fibroblasts (Figure 4A) are abundant in connective tissue and can ultimately produce collagen and the extracellular matrix (Dick et al., 2022). Since bone is composed of mostly collagen, fibroblasts play an important role in bone growth, making them a cell type of interest for bone regeneration. Skeletal myoblasts (Figure 4B) can differentiate into myocytes (muscle cells), however, if they are exposed to bone morphogenetic protein, this can cause differentiation into osteoblasts (bone cells) (Rawadi et al., 2003). This unique characteristic of skeletal myoblasts also makes them a cell type of interest in bone regeneration because of their natural regenerative properties. Both fibroblasts and skeletal myoblasts must be anchored to a surface to proliferate.

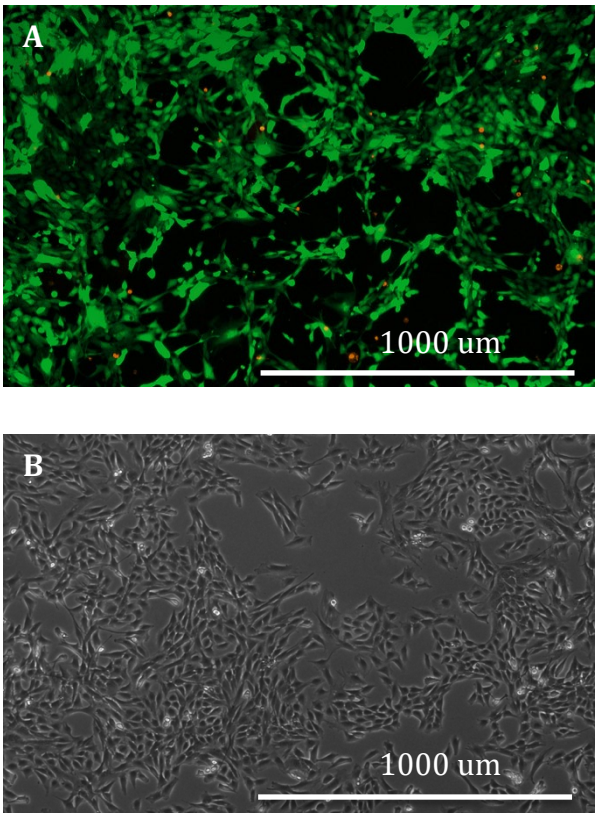

Figure 4. Cell Morphology Examples after 4 Days. **A**. GFP 3T3 Fibroblasts. **B**. C2C12 Skeletal Myoblasts.

Methods

Cells

Hydrogel cytocompatibility was evaluated by measuring mouse fibroblast (NIH3T3-GFP) and mouse skeletal myoblasts (C2C12) cell viability and growth. The NIH3T3-GFP fibroblast cell line is relatively robust and was thus used initially as a proof of concept. Experiments were then repeated and further functionalized and optimized using skeletal myoblasts, which are a better representation of eventual application to bone regeneration studies.

Cell Culture

NIH3T3-GFP fibroblast cells were cultured with DMEM Low Glucose, L-Glutamine, 10% Fetal Bovine Serum, 1% Pen/Strep cell culture media. Skeletal myoblast cells were cultured with DMEM High Glucose, L-Glutamine, 10% Fetal Bovine Serum, 1% Pen/Strep cell culture media. Cells were incubated at 37 ºC and with 5% CO_2. Prior to seeding, cells were passaged every 3-4 days, with initial seeding viabilities of above 80%. During passaging, cells were washed with phosphate buffered saline (PBS) and then after trypsin exposure, for 3 minutes at 37 ºC to encourage detachment, the trypsin was neutralized with cell culture media. Cells were spun down for 5 minutes at 0.2 RCF. The cell pellet was resuspended in fresh media, then counted and reseeded.

Cell Staining and Image Analysis

Live and dead cells were evaluated using green fluorescence from GFP or calcien AM (2.5 μM, 20 minutes) and red fluorescence from ethidium homodimer (5 μM, 20 minutes), respectively. Calcien AM stain fluorescently activates in the presence

of intracellular esterase activity. Ethidium homodimer stains the nucleus of dead cells by entering the cell through the damaged cell membrane (*LIVE/DEAD Viability/Cytotoxicity Kit*). The cells were imaged and analyzed over a period of 3 to 5 days, with a minimum of 3 time points for evaluation after seeding on the hydrogels. Live and dead cells were counted using FIJI/ImageJ analysis software.

Cell Seeding and Cytotoxicity Experiments: Polymers

Individual functionalized HA polymers were tested for cell viability and proliferation with all cell types. HA polymer, with a molecular weight of 100kDa, was dissolved according to the desired w/v% concentration then deposited into well plates. Each polymer was seeded with cells and then evaluated via cell staining and image analysis over 3-5 days of the experiment (Figure 5). HA polymers tested are as follows:

1. Oxidized HA
2. Adipic Acid Dihydrazide HA

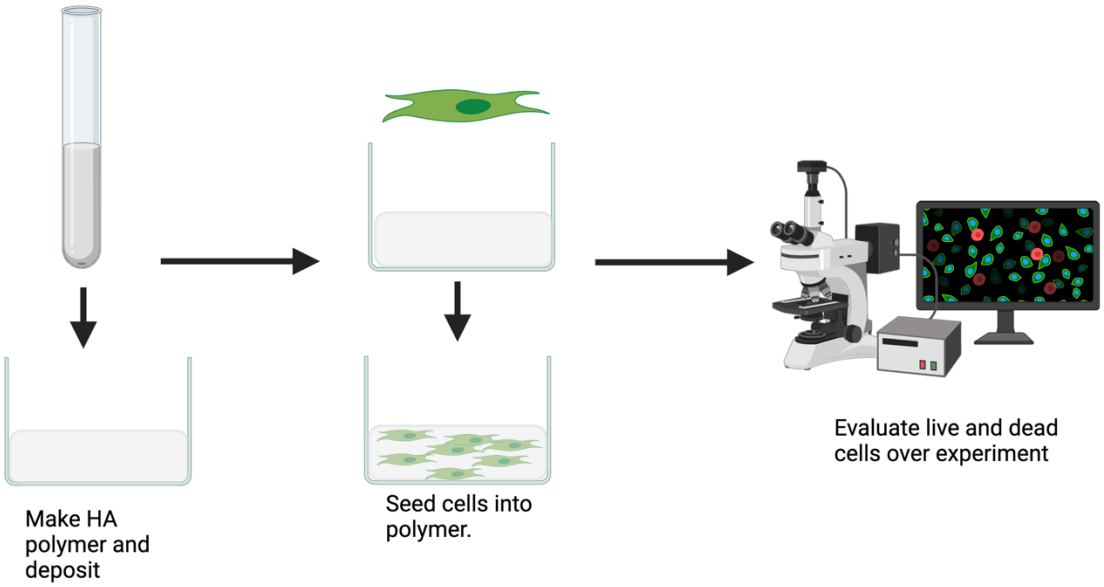

Figure 5. **Visual Depiction of Cell Seeding and Cytotoxicity Experiments with Polymers**. Figure created with BioRender.com.

3. Carbohydrazide HA

4. Pendant Diol Oxidized HA

A positive control was used, cell growth on PBS without a polymer present, to determine a baseline. The same amount of cell culture media was added to each well to provide a suitable living environment for the cells. A sample size of three per condition was used.

Hyaluronic Acid Hydrogels

HA hydrogels of varying weight percentages were formed by dynamic, covalent bonds between aldehyde functional groups on oxidized or pendant diol oxidized HA and HA functionalized with adipic acid dihydrazide or carbohydrazide groups. The chemical structures of the following four individual polymers are shown in Figure 6. Covalent crosslinking between an oxidized HA and carbohydrazide HA forms a hydrogel at room temperature over a time frame of 3 minutes to 2 hours. The individual polymers were mixed, allowed to crosslink over 30 minutes, then observed for gelation. Gelation was confirmed by shining a light on the hydrogel surface. The four hydrogels created using this method are as follows:

1. Oxidized HA and Carbohydrazide HA (OX + CH HA)

2. Oxidized HA and Adipic Acid Dihydrazide HA (OX + AD HA)

3. Pendant Diol Oxidized HA and Carbohydrazide HA (PD + CH HA)

4. Pendant Diol Oxidized HA + Adipic Acid Dihydrazide HA (PD + AD HA)

To ensure the hydrogels were suitable in viscosity, gelation and swelling, gelation time and swelling studies were performed. These polymers were created using PBS.

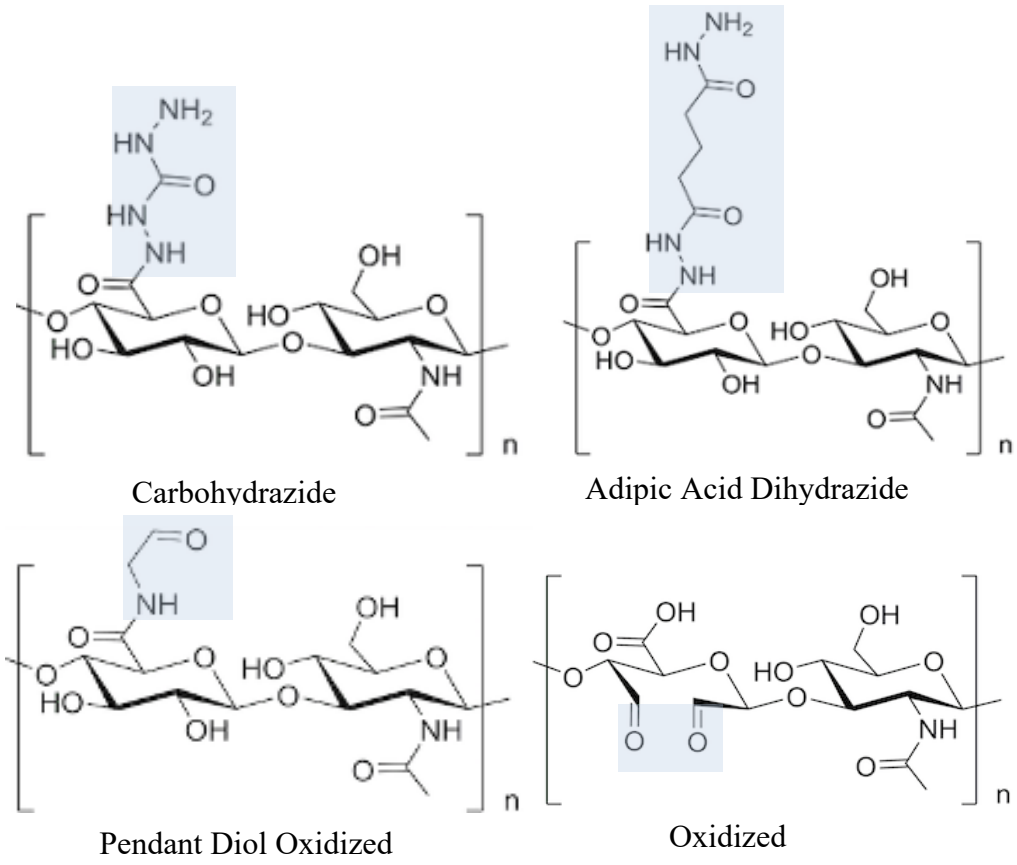

Figure 6. Molecular structure of hyaluronic acid polymers used. Highlighted blue boxes indicate the area of modification.

Cell Seeding and Cytotoxicity Experiments: Hydrogels

After the functionalized 8 µL HA polymers made with PBS were crosslinked, cell culture media was diffused into the hydrogels to create a suitable living environment for specific cell types. This was done to ensure consistent crosslinking that could not be influenced by the presence of serum proteins typically found in cell culture media. Initially, hydrogels were made with cell culture media, however after an increase in gelation time, it was hypothesized that serum proteins could be competing with aldehydes and hydrazides for binding sites. 20 µL of cell culture media was placed on the surface

of the hydrogels allowing for diffusion to happen for 20 minutes. This process was repeated three times, and once media was in the hydrogels, cells were seeded on top of the hydrogels at a density of approximately 300-400 cells/cm^2. Each hydrogel was seeded with cells and then evaluated via cell staining and image analysis over 3-5 days of the experiment (Figure 7). Cell growth on hydrogels was compared to the positive control of cell growth on the tissue culture plastic plate without a hydrogel present, to determine a baseline. A sample size of three per platform was used.

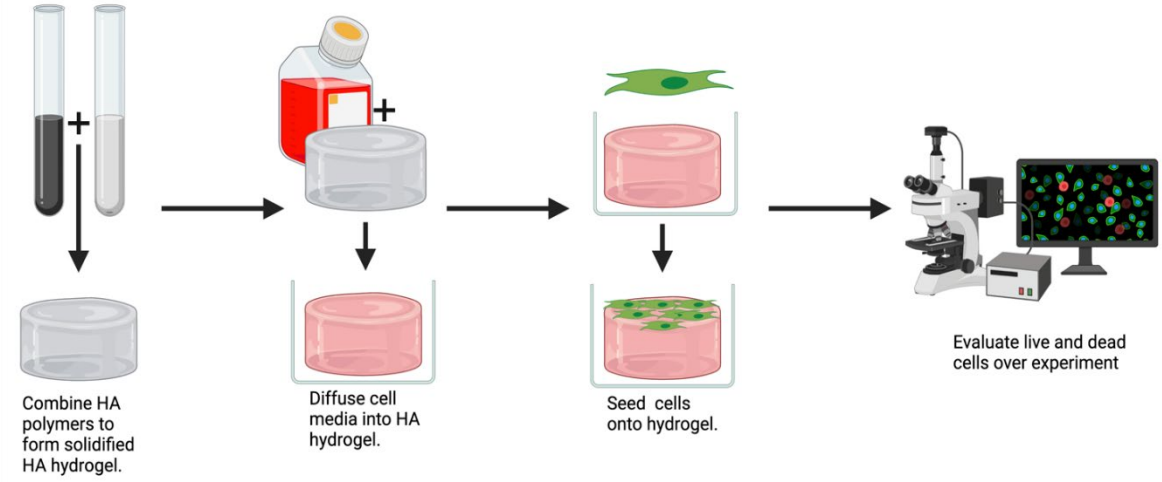

Figure 7. Visual Depiction of Cell Seeding and Cytotoxicity Experiments with Hydrogels.
Figure created with BioRender.com.

Results

Individual Hyaluronic Acid Polymer Solutions are Cytocompatible with Fibroblasts

HA dissolved in PBS to form a 2.25 w/v% solution was used to determine the cytocompatibility of modified HA polymers with fibroblasts. It was found that all

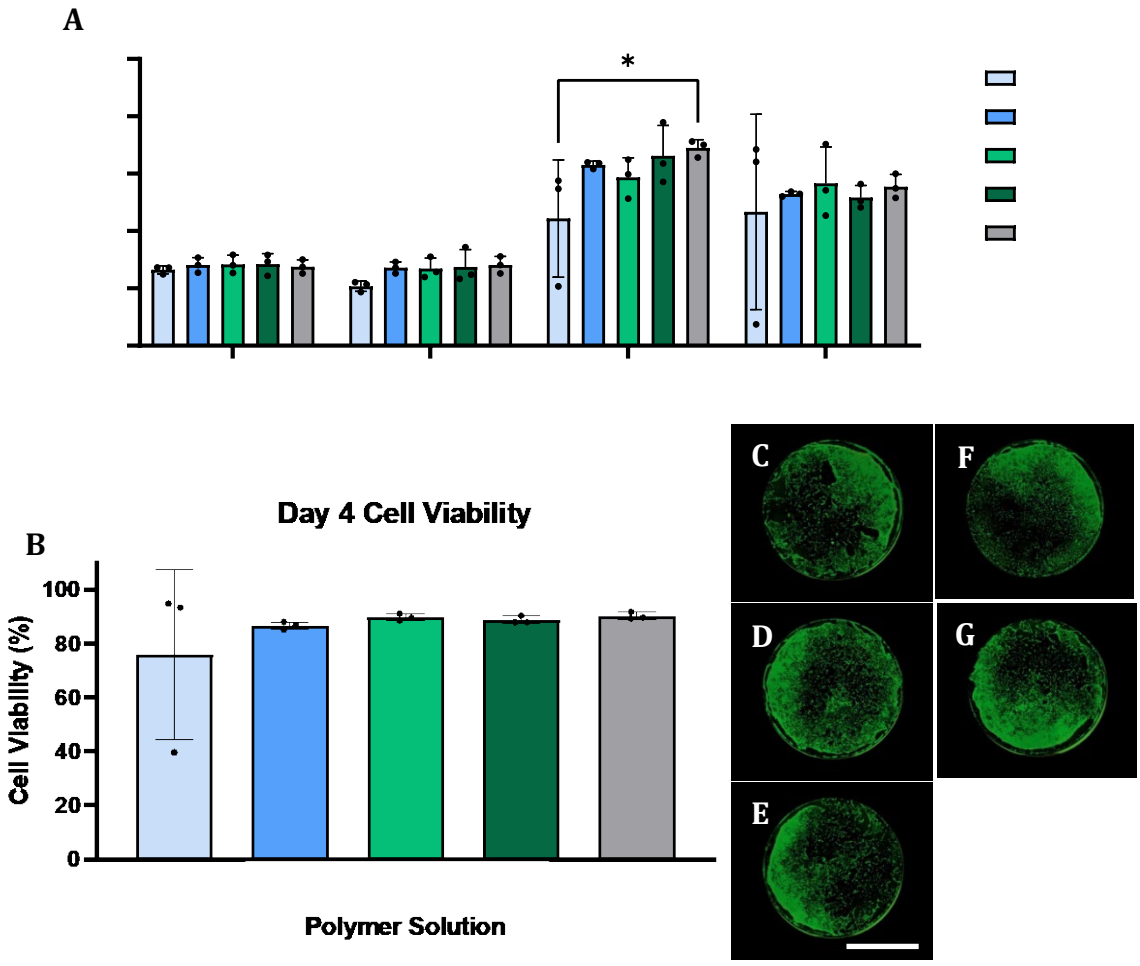

Figure 8. Individual HA Polymers are Cytocompatible with Fibroblasts. **A**. Live Cell Number Over Time. Asterisks (*) indicate $p<0.05$, 2- way ANOVA with Tukey's post- hoc test. Error bars represent standard deviations. **B**. Day 4 Cell Viability. Error bars represent standard deviation. No statistical significance found. **C-G**. Stained Cell Culture Images 4 Days After Seeding. Scale bar represents 2000 µm. **C**.OX. **D.** CH. **E**. PD. **F.** AD. **G**. PBS.

individual HA polymer solutions were cytocompatible with fibroblasts. Each condition tested showed cell viability and growth over a period of 4 days (Figure 8A and 8B) that was comparable to cells in PBS control with cell viability of greater than 80%. I hypothesize that the increased variation visible in the OX condition is due to the seeding position in the well plate. This could lead to increased evaporation and potentially cell starvation. As seen in Figure 8C-G, all conditions showed high confluency over four days of growth.

Most Hyaluronic Acid Hydrogels Support Fibroblasts

HA dissolved in PBS to form a 2.5 w/v% solution was used to determine the cytocompatibility of modified HA hydrogels with fibroblasts. It was found that all hydrogel conditions, except for PD + AD HA, support fibroblast viability and growth over five days (Figure 9A and 9B). OX + CH HA supported an increase of a 5.5-fold increase in live cells, which in comparison to the tissue culture plastic (control), only supported a 3-fold increase. PD + AD HA facilitated a decrease in live cell count of 12.9%. OX + CH HA, OX + AD HA and PD + CH HA all maintained cell viability greater than 80% for the duration of the experiment. I hypothesize that significant cell death present in PD + AD HA could be due to hydrogel degradation, inadequate anchoring surface, the presence of free aldehydes or hydrazides or a combination of the aforementioned. Figure 9C-G show varying confluency after five days of growth in different conditions.

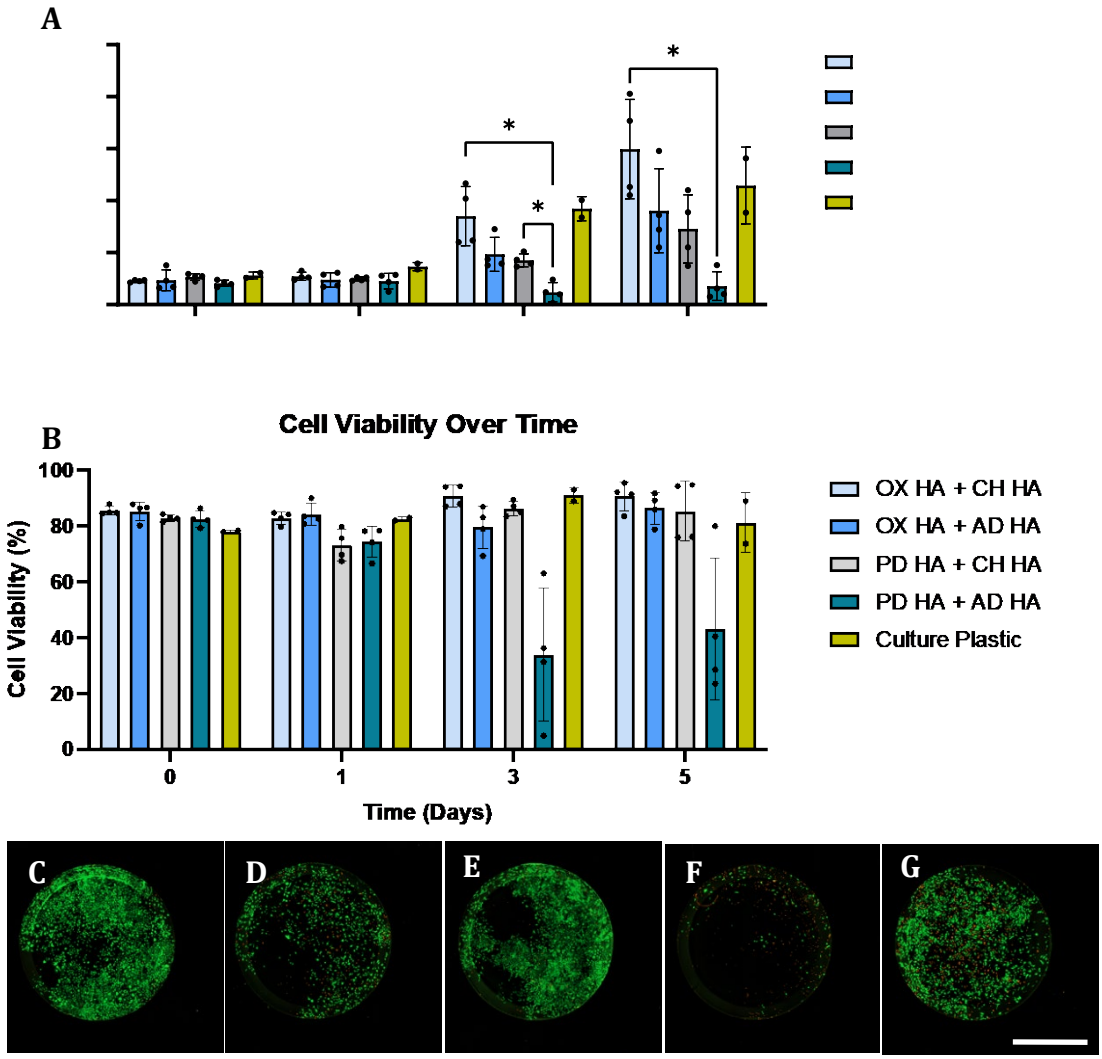

Figure 9. Most HA Hydrogels are Cytocompatible with Fibroblasts. **A**. Live Cell Number Over Time. Asterisks (*) indicate $p<0.05$, 2- way ANOVA with Tukey's post- hoc test. Error bars represent standard deviations. **B.** Cell Viability over Time. Error bars represent standard deviation. No statistical significance found. **C-G**. Stained Cell Culture Images 5 Days After Seeding. Scale bar represents 2000 µm **C**.OX + CH HA. **D**. OX + AD HA. **E.** PD + CH HA. **F.** PD + AD HA. **G**. Tissue Culture Plastic.

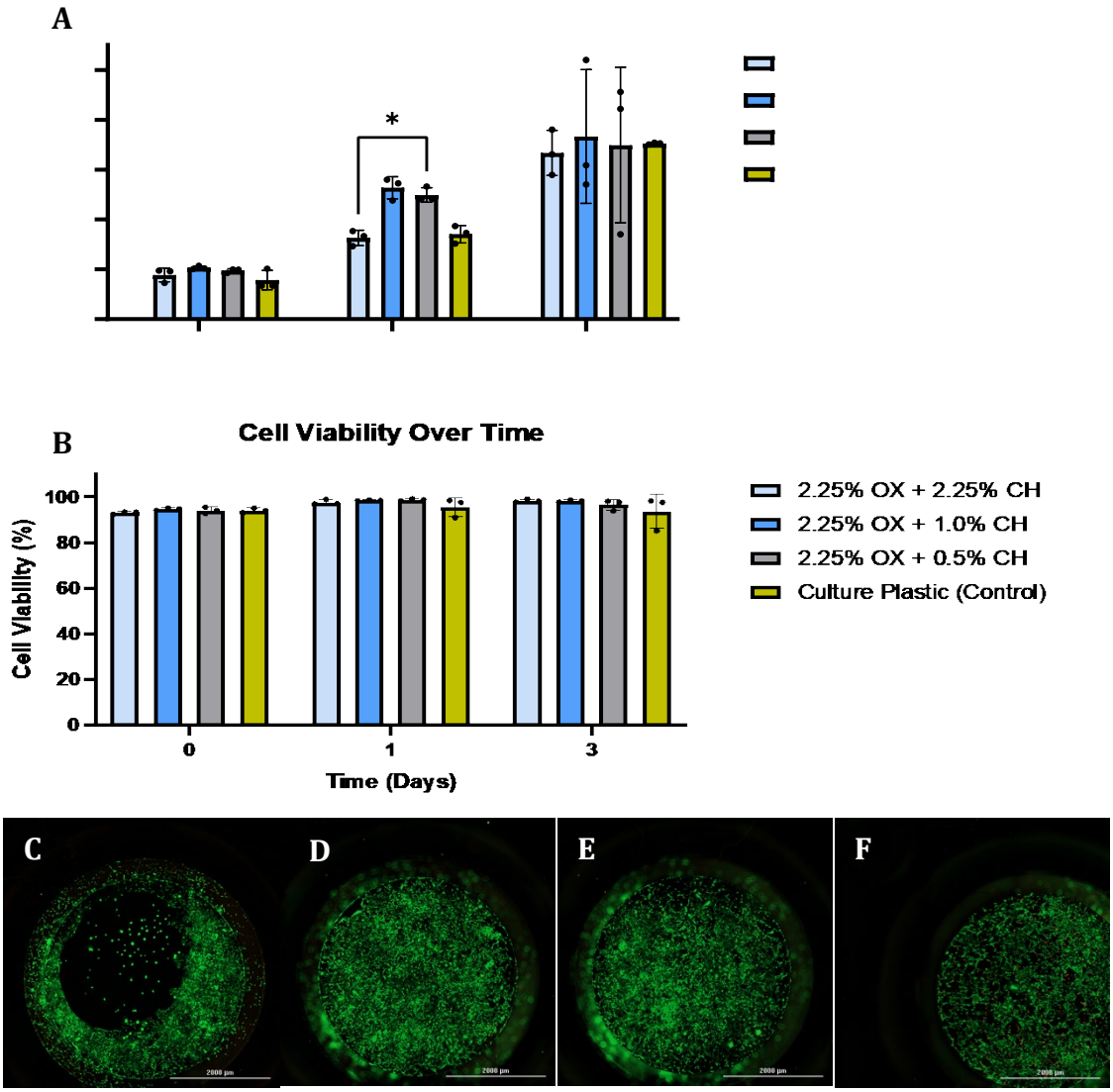

Figure 10. All OX + CH HA Platforms Support Fibroblasts. **A**. Live Cell Number Over Time. Asterisks (*) indicate $p<0.05$, 2- way ANOVA with Tukey's post- hoc test. Error bars represent standard deviations. **B.** Cell Viability over Time. Error bars represent standard deviation. No statistical significance found. **C-F**. Stained Cell Culture Images 3 Days After Seeding. Scale bars represents 2000 µm. **C**.2.25% OX + 2.25% CH HA. **D**. 2.25% OX + 1.0% CH HA. **E.** 2.25% OX + 0.5% CH HA. **F.** Tissue Culture Plastic.

Based on the previous experiment, where the OX + CH HA platform outperformed the control, we attempted to maximize proliferation using three different w/v% of the CH HA, 2.25%, 1.0% and 0.5%, while keeping the w/v% of the OX HA the same at 2.25%. When observing Figure 10A and 10B, cell growth and viability are comparable to the control with cell viabilities of greater than 88.2% and no significant (n=3) differences appearing between platforms. This indicates that the physiochemical properties of this platform could be tuned to support cell survival and proliferation in a wide range of different applications. Different w/v% have different gelation times, which can be the difference of seconds to hours. Variation in gelation time can be useful for applications that require injectability (longer gelation time) or mold creation (shorter gelation time). Figure 10C-F show varying confluency over three days of growth in different platforms. The odd cell configuration seen in Figure 10C could be due to high confluency of cells competing for limited resources.

AD + PD Hyaluronic Acid Hydrogels Do Not Support Fibroblasts

Based on the experiment where it was found that most HA hydrogels support fibroblast growth, we attempted to improve the worst performing platform the AD + PD HA using different w/v%, which are as follows, 0.5% AD + 0.5% PD HA, 2.25% AD + 0.5% PD HA, 0.5% AD + 2.25% PD HA, 2.25% AD + 2.25% PD HA, 1.37% AD + 1.37% PD HA. The data of Figure 11A and 11B, suggests that the AD + PD HA platform, regardless of optimization, does not support fibroblast proliferation. The cell growth in AD + PD HA hydrogels over time, was significantly less ($p<0.05$, $p<0.01$, $n = 3$) than the cell growth of the tissue culture plastic. Additionally, the cell viability for all hydrogel conditions decreased over time, and for most conditions cell viability was

less than 40% on the final time point (day 5) collected during the experiment. Figure 11C-H show varying confluency and morphology over five days of growth in different platforms. From these images, and correlating data in 11A and 11B, it appears that

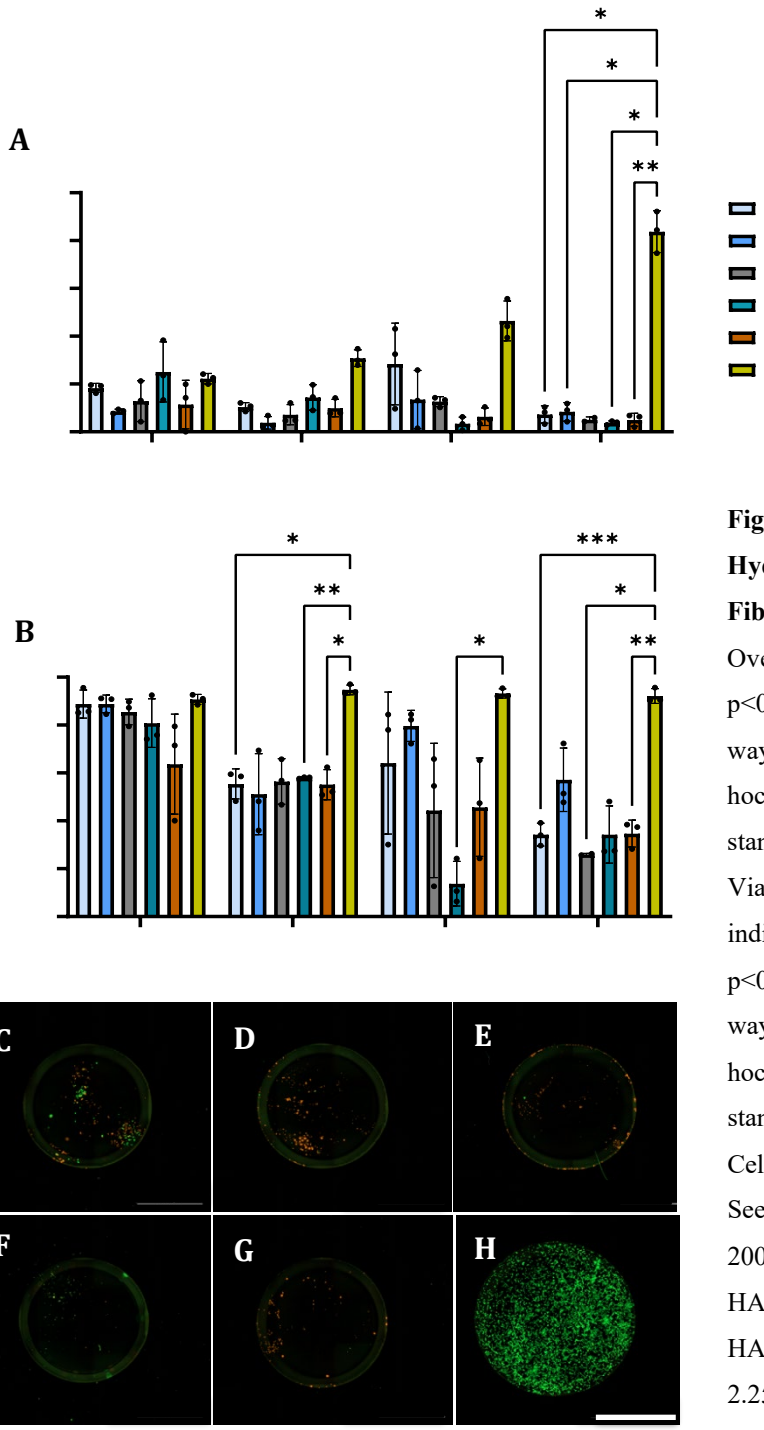

Figure 11. AD + PD HA Hydrogels Do Not Support Fibroblasts. **A**. Live Cell Number Over Time. Asterisks (*) indicate $p<0.05$, (**) indicate $p<0.01$, 2-way ANOVA with Tukey's post-hoc test. Error bars represent standard deviations. **B.** Cell Viability over Time. Asterisks (*) indicate $p<0.05$, (**) indicate $p<0.01$, (***) indicate $p<0.005$, 2-way ANOVA with Tukey's post-hoc test. Error bars represent standard deviation.. **C-H**. Stained Cell Culture Images 5 Days After Seeding. Scale bars represents 2000 µm. **C**. 0.5% AD + 0.5% PD HA. **D.** 0.5% AD + 2.25% PD HA. **E.** 1.37% AD + 1.37% PD **F.** 2.25% AD + 0.5% PD HA. **G.**

hydrogels with a lower w/v% of PD HA result in cell viabilities of less than 60% and twice as much proliferation than those with higher concentrations of PD HA. This suggests that PD HA could be causing the cytotoxicity observed in this experiment and others.

CH and OX Hyaluronic Acid Polymers are not Cytocompatible with Skeletal Myoblasts

After determining that HA polymers are cytocompatible with fibroblasts, we investigated if skeletal myoblasts, which are more in line with bone regeneration applications, are also cytocompatible with this specific platform. Using 2.25 w/v% concentrations, it was found that CH and OX individual HA polymers were not cytocompatible with fibroblasts, while AD and PD HA polymers were. AD HA, other than the PBS, performed the best regarding cell viability and cell growth after 4 days (Figure 12A and 12B). Confluency of each of the platforms can be observed in Figure 12C-G. We hypothesized that some of this death could be attributed to free aldehydes or hydrazides from uncrosslinked HA polymers, which skeletal myoblasts are more sensitive to. The presence of free aldehydes or hydrazides will be investigated by chemical analysis in future experiments to confirm the source of the problem. Since free aldehyde and hydrazide groups are reactive, we hypothesized that the hydrogel formation would improve viability.

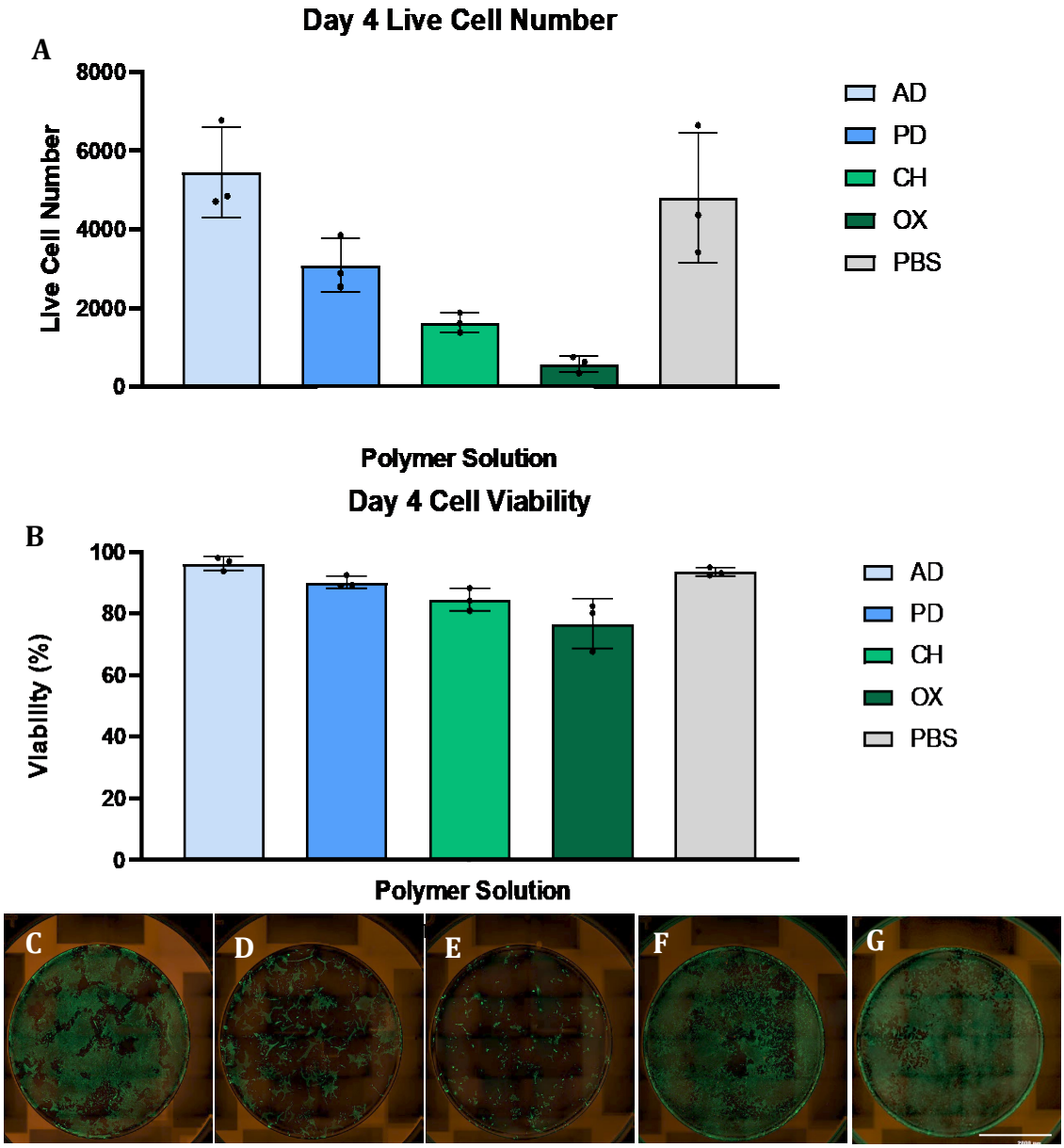

Figure 12. OX and CH HA Polymers are not Cytocompatible with Skeletal Myoblasts. A. Live Cell Number Day 4, 2- way ANOVA with Tukey's post- hoc test. Error bars represent standard deviations. **B.** Cell Viability Day 4, 2- way ANOVA with Tukey's post- hoc test. Error bars represent standard deviation. **C-H**. Stained Cell Culture Images 4 Days. Scale bars represents 2000 µm. **C**.AD HA. **D.** CH HA. **E.** OX HA. **F.** PD HA. **G.** Tissue Culture Plastic/PBS.

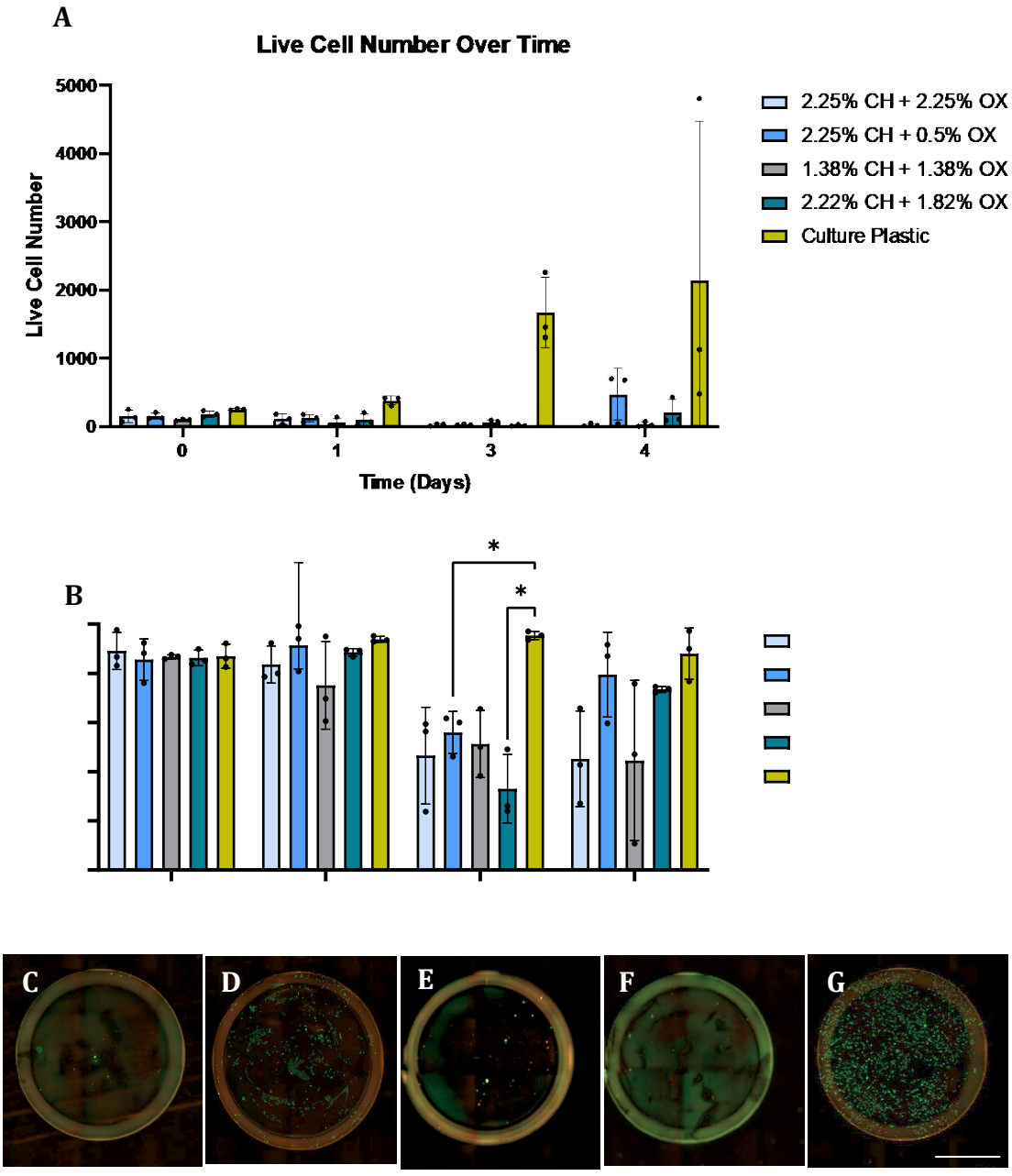

Figure 13. OX + CH HA Platform does not Support Skeletal Myoblasts. A. Live Cell Number Over Time. 2- way ANOVA with Tukey's post- hoc test. Error bars represent standard deviations. **B.** Cell Viability over Time. Asterisks (*) indicate $p<0.05$, 2- way ANOVA with Tukey's post- hoc test. Error bars represent standard deviation. **C-G**.-Stained Cell Culture Images 3 Days After Seeding. Scale bars represents 2000 µm. **C**.2.25% Ch + 2.25% OX HA. **D**. 2.25% CH + 1.0% OX HA. **E.** 1.38% CH + 1.38% OX HA. **F.** 2.22% CH + 1.82% OX. **G.** Tissue Culture Plastic.

Based on the viability and proliferation of fibroblasts on this platform, as noted in previous experiments, we aimed to determine if the best performing platform with fibroblasts could also support skeletal myoblasts. We observed different hydrogel w/v% of the CH + OX platform including, 2.25% CH + 2.25% OX HA, 2.25% CH + 0.5% OX HA, 1.38% CH + 1.38% OX + 2.22% CH + 1.82% OX HA. It was found that the CH + OX platform does not support the proliferation of skeletal myoblasts regardless of w/v% concentrations (Figure 13A and 13B). The large variability between replicates present on the day 4 of the tissue culture plastic was likely due to over confluency, which could be due to limited resources for cell survival and ultimately, death. Figure 13C-G show final confluency of each platform 4 days after initial seeding.

Hyaluronic Acid Batch Differences do not Cause an Increase in Cell Death

The reason that the OX + CH HA platform does not support skeletal myoblasts was unknown, and after the previous two experiments with very little success, we began to question if there was an impurity or issue with the newest batch of HA. Batch to batch variation of molecular weight, polymer distribution or impurities is expected in the production of HA. Purity and degree of modification of HA polymer batches were analyzed with NMR. To determine if there was a problem with the polymer, we seeded a high polymer concentration (2.25% CH + 2.25% OX HA) and low polymer concentration (0.5% CH + 0.5% OX HA) of each the old and new batch of OX and CH HA polymer and observed cell proliferation and viability over three days.

It was found that there were no significant differences between HA batches that caused a decrease in cell proliferation or viability (Figure 14A and 14B). The increased variation in cell proliferation and viability was likely due to evaporation of cell culture

media when switching to a different cell culture plate type, which caused cell death. The new cell culture plate types only held 15 wells with a surface area of 0.125 cm^2. Since the volumes of media added were in small quantities (< 60 uL), evaporation was common. The previous well plate had extra wells that PBS could be placed into to

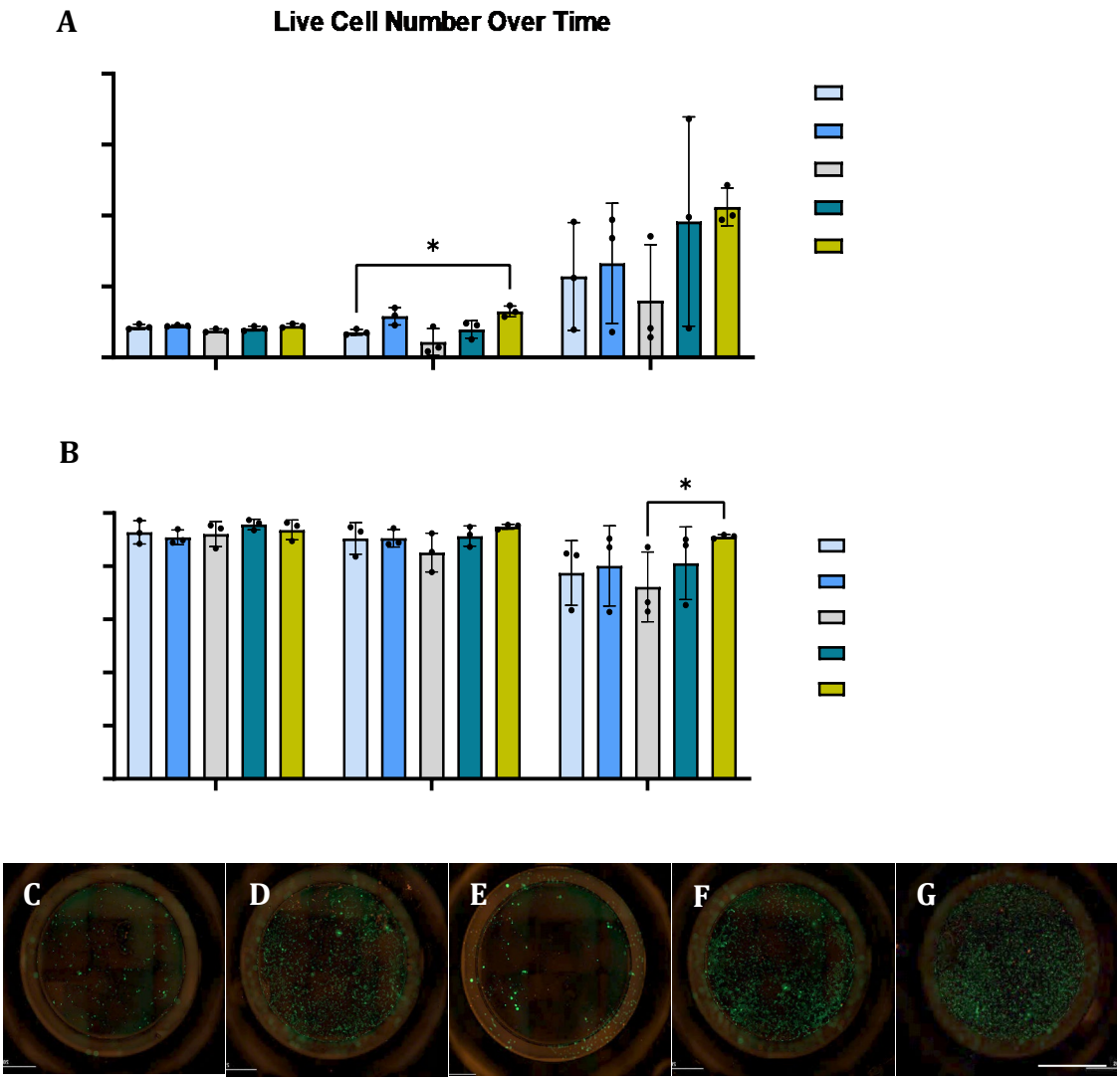

Figure 14. Hyaluronic Acid Batch Differences do not Cause an Increase in Cell Death. **A**. Live Cell Number Over Time. 2- way ANOVA with Tukey's post- hoc test. Error bars represent standard deviations. **B.** Cell Viability over Time. 2- way ANOVA with Tukey's post-hoc test. Error bars represent standard deviation. **C-G**.-Stained Cell Culture Images 3 Days After Seeding. Scale bars represents 2000 µm. **C**. New 2.25% CH + 2.25% OX HA. **D**. New 0.5% CH + 0.5% OX HA. **E.** Old 2.25% CH + 2.25% OX HA. **F.** Old 0.5% CH + 0.5% OX HA. **G.** Tissue Culture Plastic

mitigate the rapid evaporation. This was fixed in future experiments by returning to the original plate type or adding 20 uL of cell culture media to each well on days 1 and 3. Figures 14C-G show final confluency of each platform 3 days after initial seeding.

AD + OX Hyaluronic Acid Hydrogels Support Skeletal Myoblasts

We investigated an alternative platform using AD HA after concluding that the OX + CH HA platform was not suitable for skeletal myoblast proliferation. We hypothesized that this platform would prove to be more suitable, due to previous results with this HA polymer in the aforementioned experiment (Figure 12). We tested two platforms, AD + PD HA and AD + OX HA with different w/v% concentrations as follows: 2.25% AD + 2.25% PD HA, 0.5% AD.+ 0.5% PD HA, 2.25% AD + 2.25% OX HA and 0.5% AD + 0.5% PD HA. The skeletal myoblasts behaved the same as the fibroblasts for each platform. The AD + PD HA platform did not support skeletal myoblasts while the AD + OX HA platform did. The cell viability and growth after 4 days of the AD + OX HA platform was comparable to the tissue culture plastic (Figure 15). Figure 15C-G shows final confluency of each platform 4 days after initial seeding. We ultimately concluded that the AD + OX HA platform is most suitable to support cell proliferation and viability.

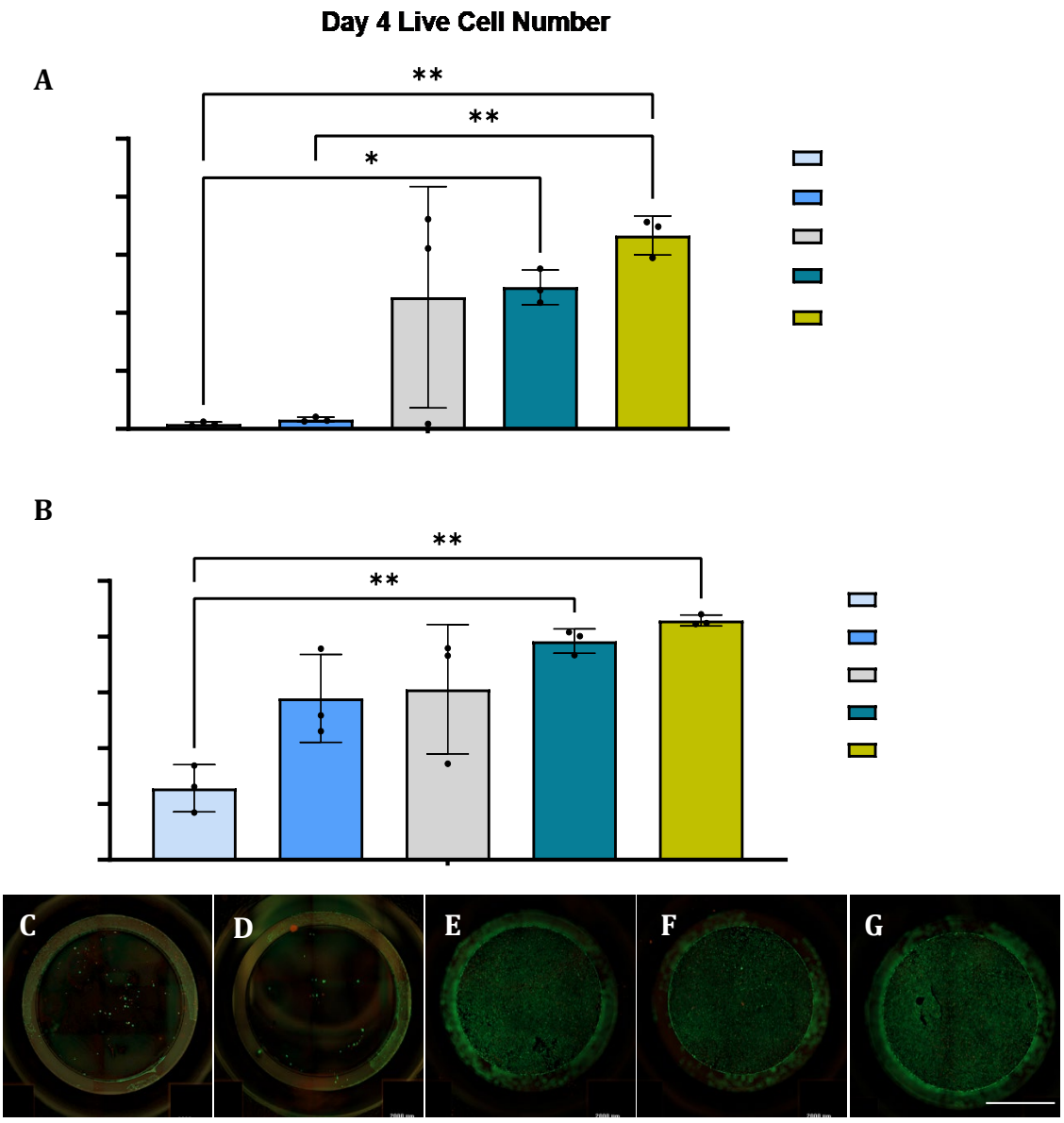

Figure 15. AD + OX HA Hydrogels Support Skeletal Myoblast. A. Live Cell Number Day 4. 2-way ANOVA with Tukey's post- hoc test. Error bars represent standard deviations. **B.** Cell Viability Day 4. 2- way ANOVA with Tukey's post-hoc test. Error bars represent standard deviation. **C-G**. Stained Cell Culture Images 4 Days After Seeding Scale bars represents 2000 µm. **C**. 2.25% AD + 2.25% PD HA. **D**. 0.5% AD + 0.5% PD HA. **E.** 2.25% AD + 2.25% OX HA. **F.** 0.5% AD + 0.5% OX HA. **G.** Tissue Culture Plastic

Discussion

Biomaterials have endless possible applications, especially in the field of regenerative medicine where specific injuries require medical intervention to heal. Hydrogels, specifically, are uniquely positioned for bone regeneration applications since they can be loaded with a variety of cells or proteins to produce a rapid osteogenic healing response (Hettiaratchi et al., 2020). Currently, hydrogels are not being used in clinical practice for regenerative medicine. However, the functionalized HA hydrogels tested in these experiments have the potential to rival the healing response of the current method for bone regeneration and replacement through further optimization and experimentation (Muir & Burdick, 2021). The development of a hydrogel that can be loaded with the necessary proteins and cells involved in the bone healing cascade to stimulate regeneration would revolutionize regenerative and reconstructive medicine. Potentially, patients who have cancerous tumors excised can have this biomaterial injected into the bone defect site to accelerate regrowth and healing (Chen et al., 2022). With a biomaterial that can mimic and function as native bone, the need for amputations could be reduced and the success rate of limb salvage could be increased (Marcinczyk et al., 2019).

In this study, we aimed to determine what functionalized form of HA polymers that form hydrogels would support the greatest degree of cell viability and proliferation for future bone regenerative applications. Through a combination of a variety of cytotoxicity experiments, we identified that the CH + OX HA platform supported fibroblasts best but was cytotoxic to skeletal myoblasts. This finding was unexpected and the exact mechanics of why this difference was observed is still unknown and

requires further experimentation. One possible reason for this difference could be that the skeletal myoblasts are unable to effectively anchor themselves to the surface of the CH + OX HA hydrogel. It is possible that the use of specific extra cellular matrix proteins, such as fibronectin or laminin, could be used to facilitate cell adhesion to the surface of the hydrogel, and thus greater proliferation (Stowers, 2022) (Chowdhury et al., 2015). We also identified that the AD + OX HA platform supported cell viability and proliferation for both skeletal myoblasts and fibroblasts. Future experiments to optimize and further functionalize this hydrogel platform are necessary.

Ideally, we would see high cell viability and growth in a variety of different w/v% platforms, which would indicate that the physiochemical properties of different platforms could be tuned to support cell survival and proliferation in a wide range of different applications. The w/v% composition of a HA hydrogel is directly correlated to the gelation rate. Cell survival in a wide range of different w/v% HA hydrogels would allow for this therapeutic technique to be injected, leading to less invasive surgeries, ultimately leading to safer and faster healing or to be formed into a mold, which could be placed and secured into a large bone-defect to promote osteogenic repair and regeneration. We also identified that the PD + AD HA hydrogel platform was cytotoxic to all cells and all w/v% concentrations tested. The lack of literature available regarding PD + AD HA hydrogels along with the results of this study, we concluded that this platform is not viable for any bone regenerative related applications.

While there was considerable variation in some of the experiments performed, additions to protocols that mitigated evaporation issues reduced error were made. Technique of cell seeding, strategic redistribution of cell culture media, and close

monitoring helped mitigate these issues. Increasing the sample size to greater than n=3 in future experiments could also lower experimental error. Overall, these experiments were reproducible and reliable for determining the cytocompatibility of these functionalized HA hydrogels.

Based on the results of this study multiple future directions could be pursued. Currently, cells are being tested for viability on the surface of hydrogels. It is possible that there is a difference in viability and proliferation when cells are seeded inside hydrogels as opposed to on top of them. Additionally, since we identified a HA hydrogel platform that supports the proliferation of fibroblasts and skeletal myoblasts further experimentation and modification to further develop them into the ideal biomaterial for bone regeneration could now be pursued. Since hydrogels can be loaded with cells and proteins, we could further modify the HA polymers to create ideal binding sites for proteins involved in the bone healing cascade (Dorogin et al., 2021).

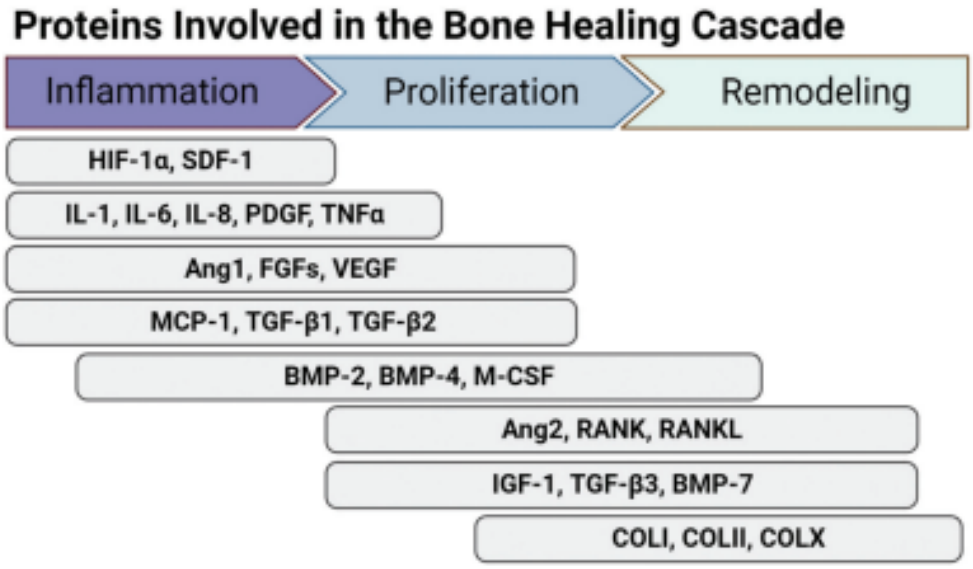

Figure 16. **A wide variety of proteins are involved in the bone healing cascade** (Dorogin et al., 2021). Figure created with BioRender.com.

This cascade is divided into three major stages, inflammation, the rush of white blood cells to the injury site, proliferation, the regeneration of blood vessels and cartilaginous tissue, and lastly remodeling, the reformation of hard bone tissue. Further engineering of the HA hydrogels into sustained protein release vehicles could allow for the hydrogels to selectively release the required proteins during the correct stage of the bone healing cascade (Figure 16). This would maximize protein usage and increase the effectiveness of the therapeutic technology. Bone morphogenetic protein 2 (BMP-2) is heavily involved in the regeneration of bone and cartilage, and since it is involved in a majority of the bone healing cascade, its encapsulation in a hydrogel would be beneficial to promoting an osteogenic response (Hettiaratchi et al., 2020). Sustained release of BMP-2 could be observed in vitro via skeletal myoblasts, which upon exposure to BMP-2 differentiate into osteoblasts (Katagiri et al., 1994.). An alkaline phosphatase assay could quantify osteoblast activity and ultimately show early bone formation.

After these cytocompatible HA hydrogels are engineered to host osteogenic proteins, like BMP-2, and have exhibited sustained release over time, these hydrogels could be implanted in vivo to observe bone regeneration in a murine model over a 12-week period. Hydrogels would be sized to unilateral femoral defects created in the model and X-ray and microCT image analysis would be performed to observe localization and bone formation over time. Additionally, the use of a polycaprolactone nanofiber mesh could be used to secure the hydrogel in the defect site. This study would further establish HA hydrogels as worthwhile strategy for bone regeneration and indicate their osteo-regenerative applications.

Overall, we have established that hyaluronic acid-based hydrogels are cytocompatible with a variety of osteogenic related cells and with further engineering, have the potential to become a biomaterial that rivals the regenerative capabilities of an autograft.

Bibliography

Antoine, E. E., Vlachos, P. P., & Rylander, M. N. (2014). Review of Collagen I Hydrogels for Bioengineered Tissue Microenvironments: Characterization of Mechanics, Structure, and Transport. *Tissue Engineering. Part B, Reviews*, *20*(6), 683–696. https://doi.org/10.1089/ten.teb.2014.0086

Awad, H. A., Zhang, X., Reynolds, D. G., Guldberg, R. E., O'Keefe, R. J., & Schwarz, E. M. (2007). Recent Advances in Gene Delivery for Structural Bone Allografts. *Tissue Engineering*, *13*(8), 1973–1985. https://doi.org/10.1089/ten.2006.0107

Barrett, A. M., Craft, J. A., Replogle, W. H., Hydrick, J. M., & Barrett, G. R. (2011). Anterior Cruciate Ligament Graft Failure: A Comparison of Graft Type Based on Age and Tegner Activity Level. *The American Journal of Sports Medicine*, *39*(10), 2194–2198. https://doi.org/10.1177/0363546511415655

Bermejo-Velasco, D., Kadekar, S., Tavares da Costa, M. V., Oommen, O. P., Gamstedt, K., Hilborn, J., & Varghese, O. P. (2019). First Aldol Cross-Linked Hyaluronic Acid Hydrogel: Fast and Hydrolytically Stable Hydrogel with Tissue Adhesive Properties. *ACS Applied Materials & Interfaces*, *11*(41), 38232–38239. https://doi.org/10.1021/acsami.9b10239

Catoira, M. C., Fusaro, L., Di Francesco, D., Ramella, M., & Boccafoschi, F. (2019). Overview of natural hydrogels for regenerative medicine applications. *Journal of Materials Science: Materials in Medicine*, *30*(10), 115. https://doi.org/10.1007/s10856-019-6318-7

Chen, S., Wang, Y., Zhang, X., Ma, J., & Wang, M. (2022). Double-crosslinked bifunctional hydrogels with encapsulated anti-cancer drug for bone tumor cell ablation and bone tissue regeneration. *Colloids and Surfaces B: Biointerfaces*, *213*, 112364. https://doi.org/10.1016/j.colsurfb.2022.112364

Chowdhury, S. R., Ismail, A. binti, Chee, S. C., Laupa, M. S. bin, Jaffri, F. binti, Mohmad Saberi, S. E., & Hj Idrus, R. B. (2015). One-Step Purification of Human Skeletal Muscle Myoblasts and Subsequent Expansion Using Laminin-Coated Surface. *Tissue Engineering Part C: Methods*, *21*(11), 1135–1142. https://doi.org/10.1089/ten.tec.2015.0015

Chrobak, M. O., Hansen, K. J., Gershlak, J. R., Vratsanos, M., Kanellias, M., Gaudette, G. R., & Pins, G. D. (2017). Design of a Fibrin Microthread-Based Composite Layer for Use in a Cardiac Patch. *ACS Biomaterials Science & Engineering*, *3*(7), 1394–1403. https://doi.org/10.1021/acsbiomaterials.6b00547

Dick, M. K., Miao, J. H., & Limaiem, F. (2022). Histology, Fibroblast. In *StatPearls*. StatPearls Publishing. http://www.ncbi.nlm.nih.gov/books/NBK541065/

Dorogin, J., Townsend, J. M., & Hettiaratchi, M. H. (2021). Biomaterials for protein delivery for complex tissue healing responses. *Biomaterials Science*, *9*(7), 2339–2361. https://doi.org/10.1039/D0BM01804J

Fu, W., Liu, Z., Feng, B., Hu, R., He, X., Wang, H., Yin, M., Huang, H., Zhang, H., & Wang, W. (2014). Electrospun gelatin/PCL and collagen/PLCL scaffolds for vascular tissue engineering. *International Journal of Nanomedicine*, *9*, 2335–2344. https://doi.org/10.2147/IJN.S61375

Haugen, H. J., Lyngstadaas, S. P., Rossi, F., & Perale, G. (2019). Bone grafts: Which is the ideal biomaterial? *Journal of Clinical Periodontology*, *46*, 92–102. https://doi.org/10.1111/jcpe.13058

Hettiaratchi, M. H., Krishnan, L., Rouse, T., Chou, C., McDevitt, T. C., & Guldberg, R. E. (n.d.). Heparin-mediated delivery of bone morphogenetic protein-2 improves spatial localization of bone regeneration. *Science Advances*, *6*(1), eaay1240. https://doi.org/10.1126/sciadv.aay1240

Hozumi, T., Kageyama, T., Ohta, S., Fukuda, J., & Ito, T. (2018). Injectable Hydrogel with Slow Degradability Composed of Gelatin and Hyaluronic Acid Cross-Linked by Schiff's Base Formation. *Biomacromolecules*, *19*(2), 288–297. https://doi.org/10.1021/acs.biomac.7b01133

Kassir, A. R., & Chakar, C. (2018). Current knowledge and future perspectives of bone replacement grafts. *International Arab Journal of Dentistry*, *9*(1), Article 1. http://ojs.usj.edu.lb/ojs/index.php/iajd/article/view/352

Katagiri, T., Yamaguchi, A., Komaki, M., Abe, E., Takahashi, N., Ikeda, T., Rosen, V., Wozney, J. M., Fujisawa-Sehara, A., & Suda, T. (1994). Bone morphogenetic protein-2 converts the differentiation pathway of C2C12 myoblasts into the osteoblast lineage. *The Journal of Cell Biology*, *127*(6 Pt 1), 1755–1766. https://doi.org/10.1083/jcb.127.6.1755

Kim, S.-J., Jang, J.-D., & Lee, S.-K. (2007). Treatment of long tubular bone defect of rabbit using autologous cultured osteoblasts mixed with fibrin. *Cytotechnology*, *54*(2), 115–120. https://doi.org/10.1007/s10616-007-9084-1

Kong, H. J., Alsberg, E., Kaigler, D., Lee, K. Y., & Mooney, D. J. (2004). Controlling Degradation of Hydrogels via the Size of Cross-Linked Junctions. *Advanced Materials (Deerfield Beach, Fla.)*, *16*(21), 1917–1921. https://doi.org/10.1002/adma.200400014

Lienemann, P. S., Lutolf, M. P., & Ehrbar, M. (2012). Biomimetic hydrogels for controlled biomolecule delivery to augment bone regeneration. *Advanced Drug Delivery Reviews*, *64*(12), 1078–1089. https://doi.org/10.1016/j.addr.2012.03.010

LIVE/DEAD Viability/Cytotoxicity Kit. (n.d.). 7.

Marcinczyk, M., Dunn, A., Haas, G., Madsen, J., Scheidt, R., Patel, K., Talovic, M., & Garg, K. (2019). The Effect of Laminin-111 Hydrogels on Muscle Regeneration in a Murine Model of Injury. *Tissue Engineering. Part A*, *25*(13–14), 1001–1012. https://doi.org/10.1089/ten.TEA.2018.0200

Muir, V. G., & Burdick, J. A. (2021). Chemically Modified Biopolymers for the Formation of Biomedical Hydrogels. *Chemical Reviews*, *121*(18), 10908–10949. https://doi.org/10.1021/acs.chemrev.0c00923

Park, H., Guo, X., Temenoff, J. S., Tabata, Y., Caplan, A. I., Kasper, F. K., & Mikos, A. G. (2009). Effect of Swelling Ratio of Injectable Hydrogel Composites on Chondrogenic Differentiation of Encapsulated Rabbit Marrow Mesenchymal Stem Cells In Vitro. *Biomacromolecules*, *10*(3), 541–546. https://doi.org/10.1021/bm801197m

Patenaude, M., Campbell, S., Kinio, D., & Hoare, T. (2014). Tuning Gelation Time and Morphology of Injectable Hydrogels Using Ketone–Hydrazide Cross-Linking. *Biomacromolecules*, *15*(3), 781–790. https://doi.org/10.1021/bm401615d

Rawadi, G., Vayssière, B., Dunn, F., Baron, R., & Roman-Roman, S. (2003). BMP-2 controls alkaline phosphatase expression and osteoblast mineralization by a Wnt autocrine loop. *Journal of Bone and Mineral Research: The Official Journal of the American Society for Bone and Mineral Research*, *18*(10), 1842–1853. https://doi.org/10.1359/jbmr.2003.18.10.1842

Schmoekel, H. G., Weber, F. E., Schense, J. C., Grätz, K. W., Schawalder, P., & Hubbell, J. A. (2005). Bone repair with a form of BMP-2 engineered for incorporation into fibrin cell ingrowth matrices. *Biotechnology and Bioengineering*, *89*(3), 253–262. https://doi.org/10.1002/bit.20168

Somersalo, A., Paloneva, J., Kautiainen, H., Lönnroos, E., Heinänen, M., & Kiviranta, I. (2014). Incidence of fractures requiring inpatient care. *Acta Orthopaedica*, *85*(5), 525–530. https://doi.org/10.3109/17453674.2014.908340

Stowers, R. S. (2022). Advances in Extracellular Matrix-Mimetic Hydrogels to Guide Stem Cell Fate. *Cells Tissues Organs*, *211*(6), 32–49. https://doi.org/10.1159/000514851

Wang, L. L., Highley, C. B., Yeh, Y.-C., Galarraga, J. H., Uman, S., & Burdick, J. A. (2018). 3D extrusion bioprinting of single- and double-network hydrogels containing dynamic covalent crosslinks. *Journal of Biomedical Materials Research. Part A*, *106*(4), 865–875. https://doi.org/10.1002/jbm.a.36323

Xu, F., Gough, I., Dorogin, J., Sheardown, H., & Hoare, T. (2020). Nanostructured degradable macroporous hydrogel scaffolds with controllable internal morphologies via reactive electrospinning. *Acta Biomaterialia*, *104*, 135–146. https://doi.org/10.1016/j.actbio.2019.12.038

Xu, J., Liu, Y., & Hsu, S.-H. (2019). Hydrogels Based on Schiff Base Linkages for Biomedical Applications. *Molecules (Basel, Switzerland)*, *24*(16), E3005. https://doi.org/10.3390/molecules24163005

Yu, L., & Ding, J. (2008). Injectable hydrogels as unique biomedical materials. *Chemical Society Reviews*, *37*(8), 1473–1481. https://doi.org/10.1039/B713009K

Schematics created with BioRender.com